Compact spatial multiplexers for mode division multiplexing

Compact spatial multiplexers for mode division multiplexing

Haoshuo Chen,[1] Roy van Uden,[1] Chigo Okonkwo,[1] and Ton Koonen[1]

[1]*COBRA Institute, Eindhoven University of Technology, Den Dolech 2, 5612 AZ, Eindhoven, The Netherlands*
[*]*h.chen@tue.nl*

Abstract: Spatial multiplexer (SMUX) for mode division multiplexing (MDM) has evolved from mode-selective excitation, multiple-spot and photonic-lantern based solutions in order to minimize both mode-dependent loss (MDL) and coupler insertion loss (CIL). This paper discusses the implementation of all the three solutions by compact components in a small footprint. Moreover, the compact SMUX can be manufactured in mass production and packaged to assure high reliability. First, push-pull scheme and center launch based SMUXes are demonstrated on two mostly-popular photonic integration platforms: Silicon-on-insulator (SOI) and Indium Phosphide (InP) for selectively exciting LP_{01} and LP_{11} modes. 2-dimensional (2D) top-coupling by using vertical emitters is explored to provide a coupling interface between a few-mode fiber (FMF) and the photonic integrated SMUX. SOI-based grating couplers and InP-based 45° vertical mirrors are proposed and researched as vertical emitters in each platform. Second, a 3-spot SMUX is realized on an InP-based circuit through employing 45° vertical mirrors. Third, as a newly-emerging photonic integration platform, laser-inscribed 3D waveguide (3DW) technology is applied for a fully-packaged dual-channel 6-mode SMUX including two 6-core photonic lantern structures as mode multiplexer and demultiplexer, respectively.

OCIS codes: (060.2330) Fiber optics communications; (060.4230) Multiplexing; (250.5300) Photonic integrated circuits.

References and links

1. R. W. Tkach, "Scaling optical communications for the next decade and beyond," Bell Labs Tech. J. **14**(4), 3–9 (2010).
2. A. D. Ellis, "The nonlinear Shannon limit and the need for new fibres," in (2012), Vol. 8434, p. 84340H–84340H–10.
3. R.-J. Essiambre and R. W. Tkach, "Capacity Trends and Limits of Optical Communication Networks," Proc. IEEE **100**(5), 1035–1055 (2012).
4. ModeGap," http://modegap.eu.
5. P. J. Winzer and G. J. Foschini, "Mode division multiplexed transmission systems," in *Optical Fiber Communication Conference*, OSA Technical Digest (online) (Optical Society of America, 2014), p. Th1J.1.
6. P. J. Winzer, "Energy-Efficient Optical Transport Capacity Scaling Through Spatial Multiplexing," IEEE Photon. Technol. Lett. **23**(13), 851–853 (2011).
7. R. Ryf, S. Randel, N. K. Fontaine, M. Montoliu, E. Burrows, S. Chandrasekhar, A. H. Gnauck, C. Xie, R.-J. Essiambre, and P. Winzer, "32-bit/s/Hz Spectral Efficiency WDM Transmission over 177-km Few-Mode Fiber," in *Optical Fiber Communication Conference* (2013).
8. H. Takahashi, T. Tsuritani, E. L. T. de Gabory, T. Ito, W. R. Peng, K. Igarashi, K. Takeshima, Y. Kawaguchi, I. Morita, Y. Tsuchida, Y. Mimura, K. Maeda, T. Saito, K. Watanabe, K. Imamura, R. Sugizaki, and M. Suzuki, "First demonstration of MC-EDFA-repeatered SDM transmission of 40 x 128-Gbit/s PDM-QPSK signals per core over 6,160-km 7-core MCF," Opt. Express **21**(1), 789–795 (2013).
9. M. D. Feuer, L. E. Nelson, K. S. Abedin, X. Zhou, T. F. Taunay, J. F. Fini, B. Zhu, R. Isaac, R. Harel, G. Cohen, and D. M. Marom, "ROADM System for Space Division Multiplexing with Spatial Superchannels," in *Optical Fiber Communication Conference/National Fiber Optic Engineers Conference 2013*, OSA Technical Digest (online) (Optical Society of America, 2013), p. PDP5B.8.

#222419 - $15.00 USD Received 16 Sep 2014; revised 14 Nov 2014; accepted 17 Nov 2014; published 15 Dec 2014

10. K. Igarashi, T. Tsuritani, I. Morita, Y. Tsuchida, K. Maeda, M. Tadakuma, T. Saito, K. Watanabe, K. Imamura, R. Sugizaki, and M. Suzuki, "1.03-Exabit/skm Super-Nyquist-WDM transmission over 7,326-km seven-core fiber," in *39th European Conference and Exhibition on Optical Communication (ECOC 2013)* (2013), pp. 1–3.
11. V. A. J. M. Sleiffer, Y. Jung, V. Veljanovski, R. G. H. van Uden, M. Kuschnerov, H. Chen, B. Inan, L. G. Nielsen, Y. Sun, D. J. Richardson, S. U. Alam, F. Poletti, J. K. Sahu, A. Dhar, A. M. J. Koonen, B. Corbett, R. Winfield, A. D. Ellis, and H. de Waardt, "73.7 Tb/s (96 x 3 x 256-Gb/s) mode-division-multiplexed DP-16QAM transmission with inline MM-EDFA," Opt. Express **20**(26), B428–B438 (2012).
12. Q. Kang, E. L. Lim, Y. Jung, F. Poletti, S. Alam, and D. J. Richardson, "Design of Four-Mode Erbium Doped Fiber Amplifier with Low Differential Modal Gain for Modal Division Multiplexed Transmissions," in *Optical Fiber Communication Conference/National Fiber Optic Engineers Conference 2013*, OSA Technical Digest (online) (Optical Society of America, 2013), p. OTu3G.3.
13. Y. Jung, S. Alam, Z. Li, A. Dhar, D. Giles, I. P. Giles, J. K. Sahu, F. Poletti, L. Grüner-Nielsen, and D. J. Richardson, "First demonstration and detailed characterization of a multimode amplifier for space division multiplexed transmission systems," Opt. Express **19**(26), B952–B957 (2011).
14. V. A. J. M. Sleiffer, Y. Jung, M. Kuschnerov, S. U. Alam, D. J. Richardson, L. Grüner-Nielsen, Y. Sun, and H. de Waardt, "Optical chopper-based re-circulating loop for few-mode fiber transmission," Opt. Lett. **39**(5), 1181–1184 (2014).
15. E. Ip, M.-J. Li, K. Bennett, Y.-K. Huang, A. Tanaka, A. Korolev, K. Koreshkov, W. Wood, E. Mateo, J. Hu, and Y. Yano, "146λx6x19-Gbaud Wavelength-and Mode-Division Multiplexed Transmission Over 10x50-km Spans of Few-Mode Fiber With a Gain-Equalized Few-Mode EDFA," J. Lightwave Technol. **32**(4), 790–797 (2014).
16. R. Ryf, N. K. Fontaine, M. Montoliu, S. Randel, B. Ercan, H. Chen, S. Chandrasekhar, A. Gnauck, S. G. Leon-Saval, J. Bland-Hawthorn, J. R. Salazar Gil, Y. Sun, and R. Lingle, "Photonic-Lantern-Based Mode Multiplexers for Few-Mode-Fiber Transmission," in *Optical Fiber Communication Conference*, OSA Technical Digest (online) (Optical Society of America, 2014), p. W4J.2.
17. E. Ip, M. Li, Y.-K. Huang, A. Tanaka, E. Mateo, W. Wood, J. Hu, Y. Yano, and K. Koreshkov, "146λx6x19-Gbaud Wavelength- and Mode-Division Multiplexed Transmission over 10x50-km Spans of Few-Mode Fiber with a Gain-Equalized Few-Mode EDFA," in *Optical Fiber Communication Conference/National Fiber Optic Engineers Conference 2013*, OSA Technical Digest (online) (Optical Society of America, 2013), p. PDP5A.2.
18. T. Kobayashi, H. Takara, A. Sano, T. Mizuno, H. Kawakami, Y. Miyamoto, K. Hiraga, Y. Abe, H. Ono, M. Wada, Y. Sasaki, I. Ishida, K. Takenaga, S. Matsuo, K. Saitoh, M. Yamada, H. Masuda, and T. Morioka, "2 x 344 Tb/s propagation-direction interleaved transmission over 1500-km MCF enhanced by multicarrier full electric-field digital back-propagation," in *39th European Conference and Exhibition on Optical Communication (ECOC 2013)* (2013), pp. 1–3.
19. S. Chandrasekhar, A. H. Gnauck, X. Liu, P. J. Winzer, Y. Pan, E. C. Burrows, T. F. Taunay, B. Zhu, M. Fishteyn, M. F. Yan, J. M. Fini, E. M. Monberg, and F. V. Dimarcello, "WDM/SDM transmission of 10 x 128-Gb/s PDM-QPSK over 2688-km 7-core fiber with a per-fiber net aggregate spectral-efficiency distance product of 40,320 km·b/s/Hz," Opt. Express **20**(2), 706–711 (2012).
20. R. Ryf, R.-J. Essiambre, A. H. Gnauck, S. Randel, M. A. Mestre, C. Schmidt, P. J. Winzer, R. Delbue, P. Pupalaikis, and A. Sureka, "Space-division multiplexed transmission over 4200-km 3-core microstructured fiber," in *Optical Fiber Communication Conference and Exposition (OFC/NFOEC), 2012 and the National Fiber Optic Engineers Conference* (2012), pp. 1–3.
21. R. Ryf, S. Randel, A. Gnauck, C. Bolle, R. Essiambre, P. J. Winzer, D. W. Peckham, A. McCurdy, and R. Lingle, "Space-division multiplexing over 10 km of three-mode fiber using coherent 6x6 MIMO processing," in *Optical Fiber Communication Conference and Exposition (OFC/NFOEC), 2011 and the National Fiber Optic Engineers Conference* (2011), pp. 1–3.
22. R. Ryf, N. K. Fontaine, and R.-J. Essiambre, "Spot-Based Mode Couplers for Mode-Multiplexed Transmission in Few-Mode Fiber," IEEE Photon. Technol. Lett. **24**(21), 1973–1976 (2012).
23. N. K. Fontaine, R. Ryf, J. Bland-Hawthorn, and S. G. Leon-Saval, "Geometric requirements for photonic lanterns in space division multiplexing," Opt. Express **20**(24), 27123–27132 (2012).
24. S. Yerolatsitis, I. Gris-Sánchez, and T. A. Birks, "Adiabatically-tapered fiber mode multiplexers," Opt. Express **22**(1), 608–617 (2014).
25. J. Carpenter and T. D. Wilkinson, "Characterization of multimode fiber by selective mode excitation," J. Lightwave Technol. **30**(10), 1386–1392 (2012).
26. A. M. J. Koonen, H. Chen, H. P. A. van den Boom, and O. Raz, "Silicon Photonic Integrated Mode Multiplexer and Demultiplexer," IEEE Photon. Technol. Lett. **24**(21), 1961–1964 (2012).
27. H. Chen, V. Sleiffer, B. Snyder, M. Kuschnerov, R. van Uden, Y. Jung, C. M. Okonkwo, O. Raz, P. O'Brien, H. de Waardt, and T. Koonen, "Demonstration of a Photonic Integrated Mode Coupler With MDM and WDM Transmission," IEEE Photon. Technol. Lett. **25**(21), 2039–2042 (2013).
28. PARADIGM," http://www.paradigm.jeppix.eu/.
29. M. Wale, J. Van der Tol, X. Leijtens, N. Grote, H. Ambrosius, M. Schell, D. Robbins, M. Smit, and E. Bente, "Generic foundry model for InP-based photonics," IET Optoelectron. **5**(5), 187–194 (2011).
30. F. M. Soares, K. Janiak, R. G. Broeke, and N. Grote, "Technology development towards a generic InP-based photonic-integration foundry," in M. F. Costa, ed. (2011), pp. 800111–800111–7.
31. R. Ryf, N. K. Fontaine, and R.-J. Essiambre, "Spot-based mode coupler for mode-multiplexed transmission in few-mode fiber," in *Photonics Society Summer Topical Meeting Series, 2012 IEEE* (2012), pp. 199–200.

#222419 - $15.00 USD Received 16 Sep 2014; revised 14 Nov 2014; accepted 17 Nov 2014; published 15 Dec 2014

32. H. Chen, V. Sleiffer, F. Huijskens, R. van Uden, C. Okonkwo, P. Leoni, M. Kuschnerov, L. Gruner-Nielsen, Y. Sun, H. de Waardt, and T. Koonen, "Employing Prism-Based Three-Spot Mode Couplers for High Capacity MDM/WDM Transmission," IEEE Photon. Technol. Lett. **25**(24), 2474–2477 (2013).
33. N. K. Fontaine, "Photonic lantern spatial multiplexers in space-division multiplexing," in *2013 IEEE Photonics Society Summer Topical Meeting Series* (2013), pp. 97–98.
34. K. M. Davis, K. Miura, N. Sugimoto, and K. Hirao, "Writing waveguides in glass with a femtosecond laser," Opt. Lett. **21**(21), 1729–1731 (1996).
35. H. Chen, N. K. Fontaine, R. Ryf, B. Guan, S. J. B. Yoo, and A. M. J. Koonen, "A Fully-packaged 3D-waveguide based Dual-Fiber Spatial-Multiplexer with Up-tapered 6-mode Fiber Pigtails," in *40th European Conference and Exhibition on Optical Communication (ECOC 2014)* (2014), p. We.1.1.4.

1. Introduction

The capacity limit of the existing single-mode fiber (SMF) based optical networks due to fiber nonlinearities has been forecasted [1–3]. Spatial division multiplexing (SDM) utilizes the last unexplored physical dimension, space, to avert the network bottleneck looming in the SMF networks [4] and aims to achieve extra high spectral efficiency per fiber. Compared to simply adding parallel SMFs, SDM can be more cost- and energy-efficient through densely integrating transponders, optical amplifiers and other network elements [5,6]. Both mode division multiplexing (MDM) deploying transverse modes guided in few-mode fiber (FMF) and the use of uncoupled fundamental modes or supermodes in multi-core fiber (MCF) are labeled as SDM solutions, which are capable to expand optical fiber capacity by opening the spatial domain next to the wavelength and time domain.

High capacity SDM, combined with WDM transmission trials are listed in Table 1, denoted as number (1) to (10) with an increasing transmission distance. In the top half of the table, all state-of-the-art SDM system trials are realized by MDM. The highest achieved spectral efficiency per fiber core for MDM is 32 bit/s/Hz [7], almost 3 times larger than the maximum capacity that can be offered by an SMF in the same distance. At the end of March 2014, combined SDM and WDM trials with a transmission distance longer than 1000km were only demonstrated with MCFs, listed in the bottom half of the table. Components for MCF based network such as multi-core erbium-doped fiber amplifier (EDFA) [8], MCF compatible reconfigurable optical add/drop multiplexer (ROADM) [9] and MCF loop [10] were demonstrated through directly upgrading the existing SMF based solutions. On the contrary to the MCF trials, although research for few-mode EDFA [11–13], few-mode re-circulation loop [14,15] and low-loss spatial multiplexer (SMUX) [16] achieved big progress recently, non-negligible mode-dependent loss (MDL) and coupler insertion loss (CIL) still exist in these elements, which limit the distance, especially in an accumulated case such as loop measurements. Therefore, it is essential to further explore MDM components with better performance.

In this paper, SMUX solutions based on mode-selective excitation, multiple-spot and photonic-lantern are analyzed through matrix representation. All three concepts are researched and experimentally verified with compact SMUX components instead of using bulky optics. First, compact SMUXes which are able to selectively excite LP_{01} and LP_{11} modes are demonstrated on both Silicon-on-insulator (SOI) and Indium Phosphide (InP) based circuits. 2-dimensional (2D) top-coupling by using vertical emitters is explored to provide the coupling interface between FMFs and integrated SMUX circuits. SOI-based grating couplers and InP-based 45° vertical mirrors are proposed as vertical emitters in each platform. Moreover, 2D top-coupling layout for selectively exciting four LP modes (LP_{01}, LP_{11}, LP_{21} and LP_{02}) is proposed and verified by simulations. Second, a 3-spot SMUX is demonstrated on an InP-based circuit, where three 45° vertical mirrors are machined by focused ion beam (FIB) etching. Third, a photonic-lantern based SMUX is demonstrated by laser-inscribed 3D waveguide (3DW) technology. The 3DW device consists of two 6-core photonic-lantern structures for mode multiplexing and demultiplexing and is fully packaged with an FMF and SMF array.

#222419 - $15.00 USD Received 16 Sep 2014; revised 14 Nov 2014; accepted 17 Nov 2014; published 15 Dec 2014

Table 1. High capacity SDM/WDM transmission trials

	Distance (km)	Capacity	Fiber type	SMUX solution	Highlight
(1)	119	73.7 Tb/s	*3-mode*	Phase plate	Few-mode EDFA [11]
(2)	177	24.6 Tb/s	*6-mode*	3DW	High spectral efficiency: 32 bit/s/Hz [7]
(3)	500	30 Tb/s	*3-mode*	Phase plate	Few-mode re-circulation loop [17]
(4)	900	9.6 Tb/s	*3-mode*	Fiber lantern	Low-loss fiber lantern coupler [16]
(5)	1000	3.5 Tb/s	*3-mode*	Phase plate	Record MDM/WDM transmission distance [17]
(6)	1500	2 344Tb/s	12-core	Fiber bundle	Nonlinear compensation [18]
(7)	2688	7.5 Tb/s	7-core	Fiber bundle	Core-to-core signal rotation [19]
(8)	4200	1.2 Tb/s	3-core	Spot coupler	3 coupled-core micro-structured fiber [20]
(9)	6160	28.8Tb/s	7-core	Fiber bundle	Multi-core EDFA [8]
(10)	7326	140.7Tb/s	7-core	Fiber bundle	Super-Nyquist WDM [10]

2. Spatial multiplexer (SMUX)

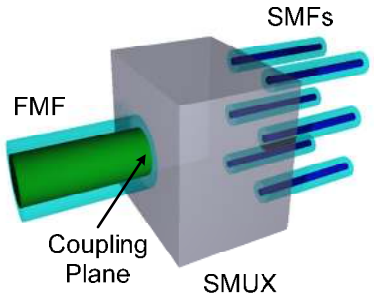

Fig. 1. Schematic diagram of the SMUX.

Figure 1 shows the schematic diagram of the SMUX, whose basic functionality is to convert optical powers from a bundle of SMFs into guided modes of an FMF. To discuss and compare different mode multiplexing solutions, matrices are utilized to represent the SMUX, as shown below:

$$\underbrace{\begin{bmatrix} F_1 \\ F_2 \\ \vdots \\ F_N \end{bmatrix}}_{F:\,mode\ field} = \underbrace{\begin{bmatrix} \gamma_{1,1} & \gamma_{1,2} & \cdots & \gamma_{1,N} \\ \gamma_{2,1} & \gamma_{2,2} & & \gamma_{2,N} \\ \vdots & & \ddots & \vdots \\ \gamma_{N,1} & \gamma_{N,2} & \cdots & \gamma_{N,N} \end{bmatrix}}_{\Gamma:\ mode\ conversion} \underbrace{\begin{bmatrix} \alpha_1 & 0 & \cdots & 0 \\ 0 & \alpha_2 & & 0 \\ \vdots & & \ddots & \vdots \\ 0 & 0 & \cdots & \alpha_N \end{bmatrix}}_{A:\ internal\ attenuation} \underbrace{\begin{bmatrix} I_1 \\ I_2 \\ \vdots \\ I_N \end{bmatrix}}_{I:\,launch\ field} \tag{1}$$

where I represents Gaussian-distributed fields from SMFs, F is an array of the fields of fiber modes guided by an FMF and N is the number of total modes. A is a diagonal matrix representing SMUX internal attenuation, which can be caused by splitters inside the device. Γ is the mode conversion matrix, which is quantified with intensity overlap integrals at the

#222419 - $15.00 USD Received 16 Sep 2014; revised 14 Nov 2014; accepted 17 Nov 2014; published 15 Dec 2014

coupling plane. The plane locates at the entry facet of the FMF, as shown in Fig. 1. The intensity overlap integral is calculated as:

$$\gamma_{i,j} = \frac{\int E^*_{launch,i} \cdot H_{mode,j} dS}{\sqrt{\int E^*_{launch,i} \cdot H_{launch,i} dS} \sqrt{\int E^*_{mode,j} \cdot H_{mode,j} dS}} \tag{2}$$

where $E_{launch,i}$ and $H_{mode,j}$ are the transverse electric field of the i^{th} launch field at the coupling plane and the transverse magnetic field of the j^{th} fiber mode, respectively. S is the fiber cross-sectional area. The notation * indicates the complex conjugate.

Then, the $N \times N$ transfer matrix of the SMUX can be represented as:

$$H = \Gamma \cdot A \tag{3}$$

For the purpose to investigate the performance of different kinds of SMUXes, the CIL and MDL are chosen and defined as:

$$CIL = \frac{\sum(\lambda_n^2)}{N} \tag{4}$$

$$MDL = \frac{\max(\lambda_n^2)}{\min(\lambda_n^2)} \tag{5}$$

where λ_n (n = *1* to N) are singular values of the SMUX transfer matrix H through employing singular value decomposition (SVD).

The phase-plate based SMUX was widely-used [21] and has the advantages such as mode-selective excitation and detection. However, due to the usage of beam combiners, the values of A in Eq. (1) are proportional to N, which results this solution is less scalable to a large mode number. Spot-based SMUX was proposed as a scalable solution, which excites a linear combination of modes instead of one specific mode [22]. Without using the lossy beam combiners, A for the spot-based SMUX can be regarded as an identity matrix and neglected. Therefore, CIL and MDL are determined only by how well spots are arranged. However, unnegligible MDL and CIL still exist for the spot-based SMUX. In order to achieve a potentially lossless solution for mode (de)multiplexing, photonic-lantern based SMUX was proposed [23,24], where N SMFs or waveguides are adiabatically tapered down into a few-mode front-end, guiding N spatial modes. For a photonic-lantern based SMUX, Eq. (1) can be simplified as:

$$\begin{bmatrix} F_1 \\ F_2 \\ \vdots \\ F_N \end{bmatrix} = \Gamma \begin{bmatrix} I_1 \\ I_2 \\ \vdots \\ I_N \end{bmatrix} = \Gamma \underbrace{\begin{bmatrix} F_1' \\ F_2' \\ \vdots \\ F_N' \end{bmatrix}}_{\substack{\text{F': front-end} \\ \text{supermodes}}} \tag{6}$$

where F' represents the supermodes at the few-mode front-end. If the supermodes match the guided modes of the FMF, Γ and A in Eq. (3) both become unitary, which gives a unitary H. In this case, lossless mode conversion is realized.

#222419 - $15.00 USD Received 16 Sep 2014; revised 14 Nov 2014; accepted 17 Nov 2014; published 15 Dec 2014

3. Compact solutions for SMUX

In this section, compact SMUX solutions based on mode-selective excitation, multiple-spot and photonic-lantern concepts are presented. Two most popular photonic integration platforms: SOI and InP, and newly-emerging femto-second laser-inscribed 3DW technology are explored for compact SMUXes, which are with small footprints, high reliability and suitable for low-cost device packaging.

3.1 Mode-selective excitation

To selectively launch one specific mode with high coupling efficiency (CE) and low crosstalk to other modes, a field as similar as possible to that of the desired mode needs to be generated [25]. Both amplitude and phase of the generated field determine CE. The LP_{01} mode field is unipolar, and the LP_{11} mode has a bipolar field distribution. A push-pull scheme was proposed to excite the LP_{11} mode where two Gaussian-like spots are used with a phase difference of π [26]. The comparison of the fields of the LP_{11a} mode and the push-pull case is shown in Fig. 2(a). With an extra spot locates at the centre, five spots are able to selectively excite and detect all three spatial modes, see Fig. 2(b). The LP_{11a} and LP_{11b} mode fields are orthogonal, and rotated $\pi/2$ with respect to each other in the FMF cross-section area.

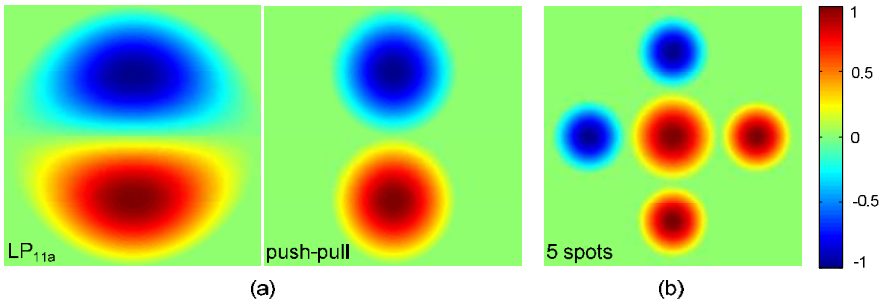

Fig. 2. (a) Comparison of the fields of the LP_{11a} mode and push-pull case; (b) 5-spot region.

3.1.1 SOI-based grating coupler

Edge-coupling by a spot-size convertor (SSC) or lensed fiber, and top-coupling by a grating coupler are the dominant approaches for coupling between an SOI-based photonic integrated circuit and an SMF. However, it is challenging for the edge-coupling to stack multiple waveguide layers together with a small spacing to realize 2D coupling for SDM, especially for coupling into an FMF, where 2D patterns need to be positioned in a micrometer accuracy. Top-coupling gives more freedom through arranging vertical emitters in 2D. For the purpose of MDM, small grating couplers based on SOI are designed for coupling into FMFs without the use of imaging optics. In order to create a bipolar field for LP_{11} mode excitation, two 2D grating couplers are driven in a push-pull configuration with opposite phase [26]. To further extend this concept, a full 6-channel integrated SMUX is sketched in Fig. 3(a), where the center 2D grating coupler is for launching or detecting the LP_{01} mode. The SMUX connects 6 individual SMFs through one-dimensional grating couplers to five 2D grating couplers for FMF coupling. The five small 2D vertical grating couplers excite 6 mode channels: the x- and y-polarization of the LP_{01} and of the degenerate LP_{11} modes (LP_{11a} and LP_{11b}). A scanning electron microscope (SEM) image of the region with vertical grating couplers are shown in Fig. 3(b). One integrated SMUX has been packaged with an SMF array for 6 SMF ports and wire-bonded to an electronic circuit, see Fig. 3(c).

A short step-index (SI) FMF with a core size of 19.4μm is used to test the packaged SMUX. Figure 4(a) shows the launched mode profiles when adding optical power into each SMF input port individually. Voltage is applied to the heater for fine-tuning the phase as

#222419 - $15.00 USD Received 16 Sep 2014; revised 14 Nov 2014; accepted 17 Nov 2014; published 15 Dec 2014

launching pure LP_{11} modes and no phase tuning is needed for LP_{01} modes excitation. Figure 4(b) shows the measured insertion losses versus wavelength for all 6 channels when the SMUX is used as a mode multiplexer. 20dB insertion loss for the LP_{01} mode is achieved. The insertion loss for an SMF-to-SMF self-loop including two 1D grating couplers is plotted as a blue curve in Fig. 4(b). It can be calculated that the coupling loss from an SMF to a waveguide via the 1D grating coupler is around 4dB. Besides on-chip losses, main loss comes from the small vertical grating couplers which are with a design of 5 periods. The few period design lowers the light diffraction efficiency of the grating and thus induces a quite high loss. Due to the limited space, the large spacing between the pairs of grating couplers causes more loss for LP_{11} mode excitation than the LP_{01} mode excited by the single grating coupler at the centre. By employing the proposed SOI SMUX, 3.072Tb/s (6 spatial and polarization modes×4 WDM×128Gb/s 16QAM) transmission over 30km 3-mode FMF was achieved [27].

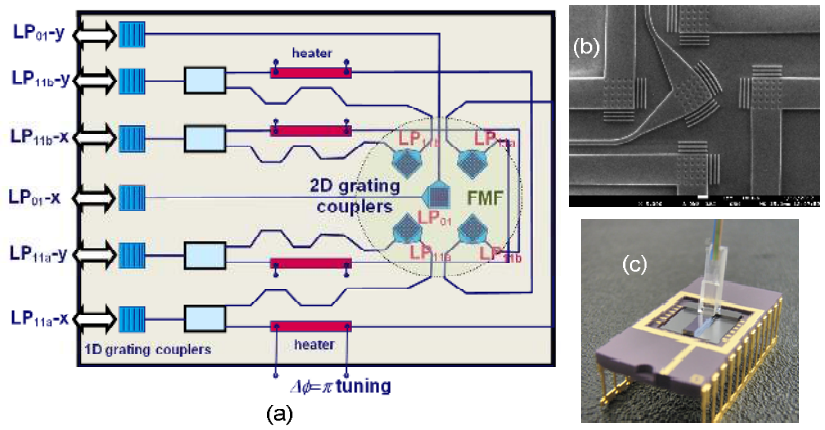

Fig. 3. (a) Circuit schematics, (b) SEM image of the region of five grating couplers, (c) image of the packaged SOI-based SMUX.

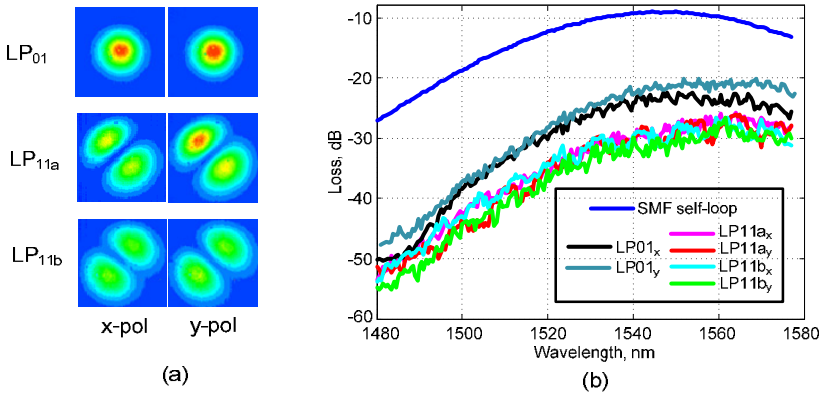

Fig. 4. (a) Excited mode profiles for all spatial modes in two polarizations and (b) insertion loss for LP_{01} and LP_{11} modes versus wavelength.

3.1.2 InP-based 45° vertical mirror

45° vertical mirror based on total internal reflection (TIL) of the surface between a high-index waveguide and air is introduced as a vertical emitter for 2D top-coupling, which is suitable for InP platform. Vertical mirror has a wider bandwidth than the SOI-based grating coupler, which is wavelength dependent due to its periodic structure. The schematic of the 45° mirror is shown in Fig. 5(a). TIR happens at the slanted boundary of air and high-index waveguide.

#222419 - $15.00 USD Received 16 Sep 2014; revised 14 Nov 2014; accepted 17 Nov 2014; published 15 Dec 2014

InP-based platform under PARADIGM project [28] is chosen due to its high availability of both active and passive building blocks [29,30]. To deduce the loss from Fresnel diffraction at the top, anti-reflection (AR) layer can be coated. The mirror fabrication is done through focused Ion beam (FIB) etching. The SEM image of a 45° vertical mirror fabricated on an InP waveguide with a width of 4μm is shown in Fig. 5(b). It is measured that coupling loss from the vertical mirror to an SMF is less than 9dB including 1.5dB loss from the Fresnel reflection without the usage of AR coating. Moreover, the power change is less than 0.5dB as varying the state of polarization of input light, which means the mirror is compatible with polarization division multiplexing.

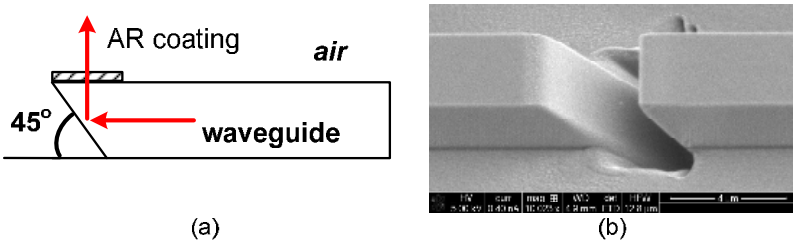

Fig. 5. (a) Schematic of the 45° vertical mirror; (b) SEM image of a 45° mirror etched on an InP waveguide.

Figure 6(a) shows the microscope image of a mode-selective excitation SMUX based on InP for LP_{01} and LP_{11} modes. The layout of 5 spots, see Fig. 2(b) is realized in the SMUX, where vertical mirrors replace the grating couplers for top-coupling. One mirror located at the center is for launching or detecting LP_{01} modes. Four mirrors in a outer ring with a radius around 6.8μm are for LP_{11} modes (LP_{11a} and LP_{11b}) selective excitation. For LP_{11} mode channel, light is split by a multi-mode interferometer (MMI) based 1×2 splitter. The thermo-optic effect based phase tuner is applied to fine-tune the phase change in one waveguide arm to create the π phase difference for push-pull output. Deeply-etched waveguides with a width of 2μm and etch depth of 1.7μm are used for the mirrors. The mirror machining is done with two FIB fabrication steps: a raw round scan and a fine line scan. It takes 3 minutes for the 1st round scan etching with an acceleration voltage of 30kV and a beam current of 26pA and 4 minutes for the final line scan etching with 9pA. For an SI-FMF with a core diameter of 19.3μm [27], 4% and 7% CE is achieved by simulations for LP_{01} and LP_{11} modes, respectively, which results in 3dB MDL and 12 dB CIL. Atoms redeposition on the center waveguide can be observed from the comparison of Figs. 6(b) and 6(c), which is normal in the FIB nanofabrication process. An SEM image of the region with the 5 fabricated mirrors is shown in Fig. 6(d).

#222419 - $15.00 USD Received 16 Sep 2014; revised 14 Nov 2014; accepted 17 Nov 2014; published 15 Dec 2014

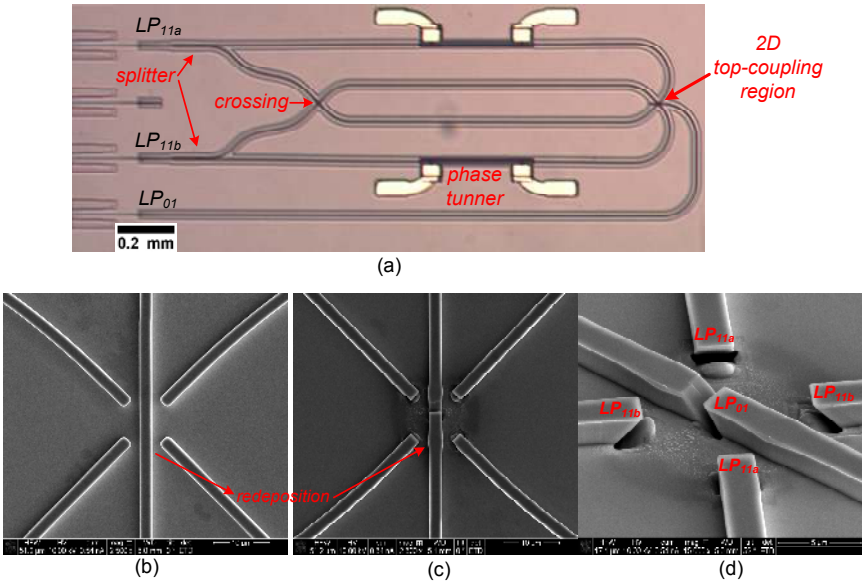

Fig. 6. (a) Microscope image of an InP-based SMUX circuit; SEM images of the 5-spot region (b) before and (c)-(d) after mirror machining.

3.1.3 High-order modes excitation

This section scales up the mode-selective excitation solution to support four LP modes: LP_{01}, LP_{11}, LP_{21} and LP_{02}. In the view of spatial modes, there are in total 6 spatial modes which each can have two polarization states, translating into 12 transmission channels.

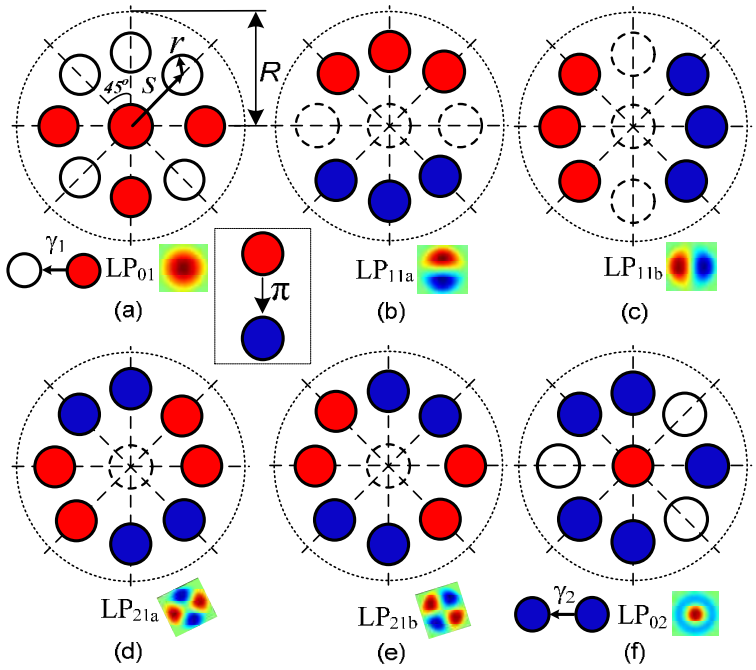

Fig. 7. The arrangement of 9 spots for selectively exciting each spatial mode.

#222419 - $15.00 USD Received 16 Sep 2014; revised 14 Nov 2014; accepted 17 Nov 2014; published 15 Dec 2014

Figure 7 illustrates the arrangement of 9 spots for selectively exciting each spatial mode which is proposed for the first time. R is the radius of an SI-FMF, guiding 6 spatial modes. All spots have a radius of r and 8 spots are uniformly distributed along a circle with a radius of s. The push-pull scheme is further developed to support LP_{11} modes, see Figs. 7(b) and 7(c) and LP_{21} modes, see Figs. 7(d) and 7(e). Unlike the 6-spot arrangement of a spot-based SMUX [31], by using more spots, a high mode extinction ratio is achieved at the same time with excellent mode CE. Due to the circular symmetry of LP_{01} and LP_{02} modes, large mode coupling happens with improper launching conditions. Through properly positioning the spots and allocating different intensities and phases to the center spot and outer 8 spots, see Figs. 7(a) and 7(f), the mode profiles of LP_{01} and LP_{02} can be nicely matched. In LP_{01} launch condition, the simulated CE for LP_{01} and LP_{02} mode is shown in Fig. 8, with $\alpha = 0.28$ and variation β and γ_1, where $\alpha = r/R$, $\beta = s/R$. γ_1 is defined as the ratio of the intensity of each spot arranged in the outer ring to that of the center one. As $\beta = 0.6$ and γ_1 is around 0.4, >60% LP_{01} mode CE is achieved and meanwhile no crosstalk to LP_{02} mode. In LP_{02} launch condition as shown in Fig. 7(f), >60% CE can also be achieved with $\beta = 0.6$ and $\gamma_2 = 0.2$, see Fig. 9. Figures 10(a) and 10(b) show the CE for LP_{11a} and LP_{21a} mode with corresponding launch condition, respectively, where all the spots share the same intensity but are with different phases. It can be seen that as $\beta = 0.6$ and $\alpha = 0.28$, four LP modes can be selectively excited with around 60% CE, which means less than 2.3dB coupling loss and no mode crosstalk to the other modes in theory due to the mode orthogonality.

This proposed SMUX has the advantage in mode selectivity at the cost of more complicated circuit design. For simultaneously exciting all modes, optical splitters, phase shifters and combiners are needed to feed each spot with combined optical signals carrying a proper intensity and phase, as illustrated in Fig. 7. To guarantee the high mode extinction ratio, optical fibers or waveguides which deliver the light to the spots cannot couple with each other. SOI- and InP-based optical waveguides are with a high core-cladding index contrast, which enables negligible waveguide crosstalk even in several micrometer gap. Due to the small size of 45° vertical mirrors and premium optical building blocks such as splitters and phase shifters in InP-based platform, InP-based SMUX with 45° vertical mirrors are potentially able to realize the complex structure as shown in Fig. 7.

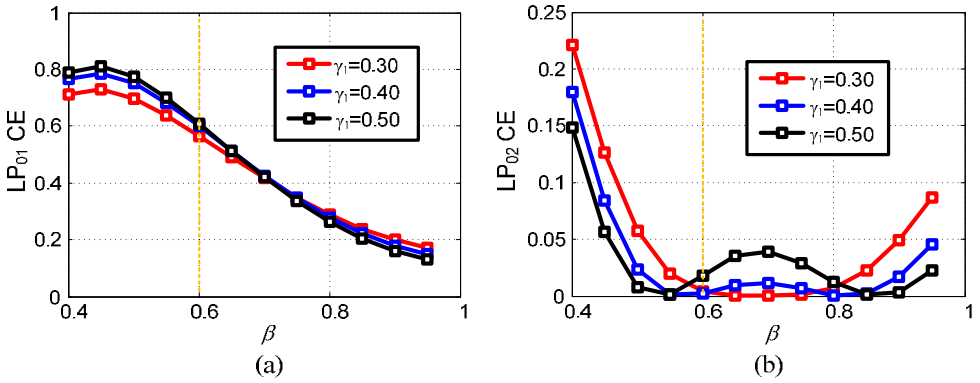

Fig. 8. CE for (a) LP_{01} and (b) LP_{02} modes under LP_{01} launch condition with $\alpha = 0.28$ and variation β and γ_1.

#222419 - $15.00 USD Received 16 Sep 2014; revised 14 Nov 2014; accepted 17 Nov 2014; published 15 Dec 2014

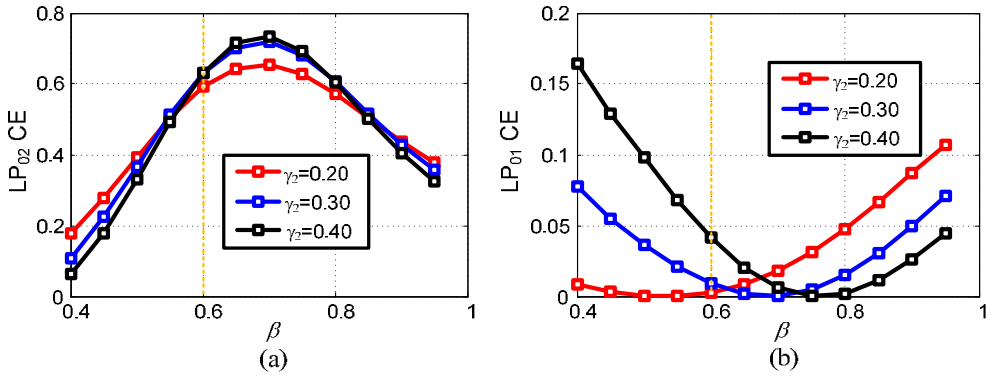

Fig. 9. CE for (a) LP_{01} and (b) LP_{02} modes under LP_{02} launch condition with α = 0.28 and variation β and γ_2.

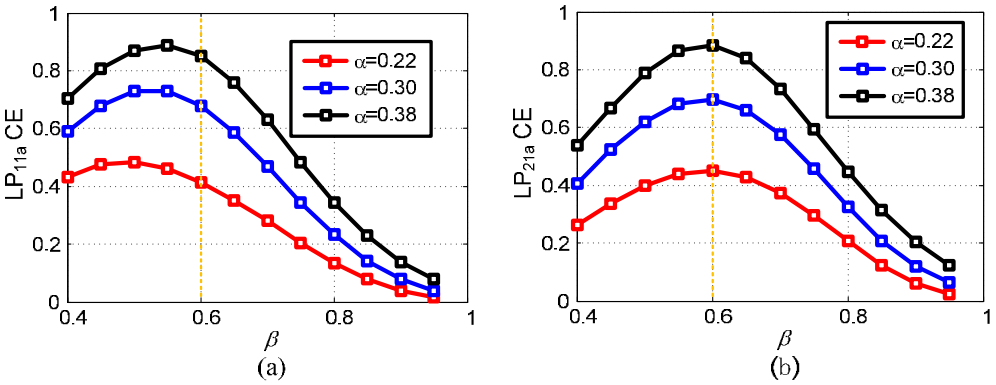

Fig. 10. CE for (a) LP_{11a} and (b) LP_{21a} modes under corresponding launch condition with variation α and β.

3.2 Spot-based SMUX

3-spot SMUX is able to provide efficient mode (de)multiplexing for LP_{01} and LP_{11} modes through locating 3 launch spots at vertices of an equilateral triangle [32], as shown in Fig. 11(a). The microscope image of a 3-spot SMUX based on InP before mirror etching in FIB post-processing is shown in Fig. 11(b). Left part of the circuit consists of five SSCs for edge-coupling with an SMF array. The purpose of two extreme channels in a loop is to ensure accurate SMF facet alignment. Figure 11(c) shows the SEM image of the merged waveguide region for 3 vertical mirrors. Medium-contrast waveguides with a width of 2μm and etch depth of 0.6μm are used for all three waveguides, which behave single-mode. Top view of the 3-spot region with the etched 45° mirrors is shown in Fig. 11(d). Figure 11(e) gives the SEM image for side view with a tilt of 52°. To acquire best surface roughness for the mirror surface, an acceleration voltage of 30kV and a beam current of 9pA is applied for the 1st round scan etching and the lowest-available beam current of 1.5pA is used for the final line scan etching. The three fabricated 45° vertical mirrors are positioned in a circle with a radius around 3.75μm. With coupling to a low differential-group-delay (DGD) 3-mode FMF [32], it is simulated that the 3-spot SMUX can achieve an MDL of 0.7dB and CIL of 9.8dB. Swept-wavelength interferometer [33] and digital signal processing will be applied to acquire measured results in future work. It should be noticed that Fresnel refraction is not considered on the assumption that AR coating or index-matching epoxy is applied. The MDL and CIL can be further minimized by optimizing the mode profile of the waveguide for mirror

#222419 - $15.00 USD Received 16 Sep 2014; revised 14 Nov 2014; accepted 17 Nov 2014; published 15 Dec 2014

machining, which can be realized through modifying waveguide's layer stack and using adiabatic taper to upscale the waveguide width.

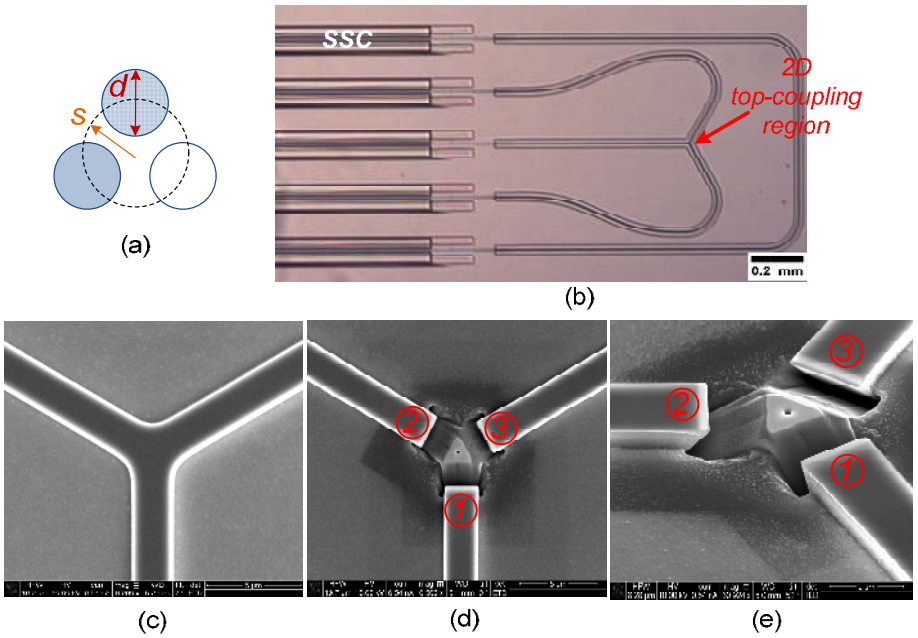

Fig. 11. (a) Spots arrangement of a 3-spot SMUX; (b) microscope image of a 3-spot SMUX circuit; SEM images of the 3-spot region (c) before and (d)-(e) after mirror machining.

3.3 3DW photonic-lantern SMUX

In order to achieve a compact and lossless mode (de)multiplexing solution, photonic-lantern based SMUX that merges N single mode waveguides into a few-mode waveguide that supports N spatial modes was proposed in [23] and experimentally verified in [33]. Femto-second laser-inscribed 3DW technology enables inscription of many compact waveguides into a transparent substrate [34], which is ideal to build the photonic-lantern SMUX for coupling between an SMF array on a 1-dimensional pitch to an FMF with a 2D mode pattern [35]. Figures 12(a) and 12(b) show the spot arrangement and the sketch of a 6-core photonic lantern coupling to a 6-mode FMF. In theory optical building blocks such as splitter and arrayed waveguide grating (AWG) can be realized by 3DW technology, which makes this technology potentially can be a photonic integration solution similar as SOI and InP.

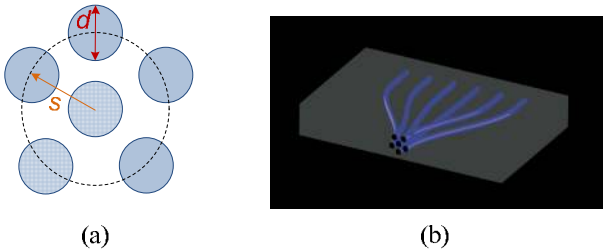

Fig. 12. (a) Spot arrangement and (b) sketch of a 6-core photonic lantern for mode multiplexing.

In this section, a fully-packaged dual-channel 6-mode SMUX is discussed, which is with two 6-core photonic-lantern structures. Therefore, mode multiplexing and demultiplexing can be realized by a single device. Figure 13(a) shows the sketch of the fully-packaged 6-mode

#222419 - $15.00 USD Received 16 Sep 2014; revised 14 Nov 2014; accepted 17 Nov 2014; published 15 Dec 2014

device. Two adiabatically up-tapered 6-mode FMFs with a cladding of 175μm are positioned and assembled in a standard V-groove. SMF array, 3DW device and FMF array are glued together using UV curing epoxy. The mode profile mismatch between the photonic lantern and FMF is solved by up-tapering FMF [35]. The packaged 3DW SMUX has a CIL less than 4dB and an MDL around 3.5dB for each photonic lantern. The picture of the fully-packaged SMUX is shown in Fig. 13(b).

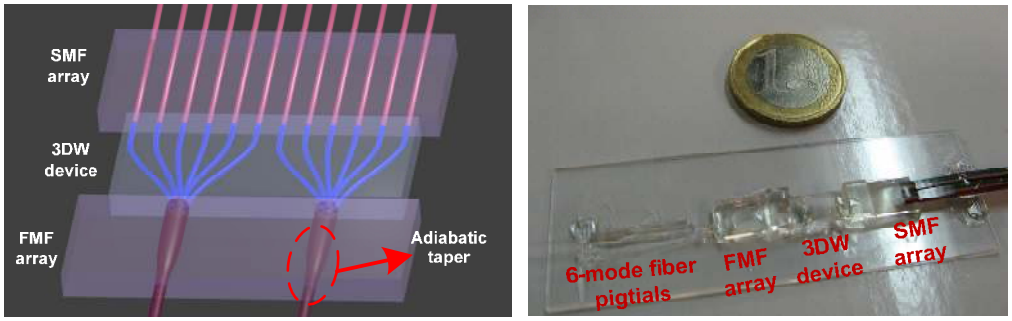

(a) (b)

Fig. 13. (a) Sketch and (b) picture of the fully-packaged dual-channel 6-mode SMUX realized by 3DW technology.

4. Conclusion

Four different compact SMUXes based on SOI platform, InP platform, and 3DW technology were investigated. To selectively excite LP_{01} and LP_{11} modes, a 5-spot layout, extended from the push-pull scheme was realized in both SOI and InP platforms. SOI-based grating couplers and InP-based 45° vertical mirrors were proposed as vertical emitters for FMF-and-circuit vertical coupling. 45° vertical mirrors were machined by FIB etching in post-processing. Subsequently, a 3-spot SMUX was presented based on InP-based 45° vertical mirrors. In order to achieve lossless mode (de)multiplexing, a 3DW SMUX was discussed, which includes two 6-core photonic-lantern structures. The fully-packaged 3DW device gave a measured MDL of 3.5dB and CIL of 4dB for each photonic lantern coupling to an up-tapered 6-mode FMF.

Acknowledgment

This work was supported in part by the European Union FP7 program BROWSE 10015285, the European Union FP7-ICT MODE-GAP project under grant agreement 258033 and the IT R&D program of MKE/KEIT (10043383, Research of Mode-Division Multiplexing Optical Transmission Technology over 10 km Multi-Mode Fiber). We acknowledge help and valuable discussions from Vincent Sleiffer, Barcones Campo, Kevin Williams and Oded Raz with Eindhoven University of Technology; Nicolas K. Fontaine, Roland Ryf with Bell Laboratories, Alcatel-Lucent; Bradley Snyder and Peter O'Brien with Tyndall National Institute, University College Cork. The SOI circuit was fabricated in the framework of ePIXfab set-up by CEA/LETI. The InP circuits were fabricated in PARADIGM multi-project wafer run by Fraunhofer HHI.

#222419 - $15.00 USD Received 16 Sep 2014; revised 14 Nov 2014; accepted 17 Nov 2014; published 15 Dec 2014